AIAA JOURNAL
Vol. 43, No. 11, November 2005

Impact Damage in Fiber Metal Laminates, Part 1: Experiment

Jeremy F. Laliberté*
National Research Council, Ottawa, Ontario K1A 0R6, Canada
Paul V. Straznicky†
Carleton University, Ottawa, Ontario K1S 5B6, Canada
and
Cheung Poon‡
Ryerson University, Toronto, Ontario M5B 2K3, Canada

Fiber metal laminates (FMLs), a new type of material for use in airframes, are composed of thin plies of metals and fiber-reinforced polymers (FRP). One drawback of conventional composite materials containing only FRP plies is their susceptibility to suffer internal damage due to low-velocity impact while showing little evidence of damage on the surface. Research reported in Part 1, and its companion Part 2, evaluated the resistance of a specific type of FML, glass-reinforced aluminum (Glare), to low-velocity impact. The experiments, a review of previous impact tests, the test program carried out in this project, and its results are discussed. The work confirmed that some consequences of impact on Glare are similar to the damage modes found in FRP composites such as delaminations, fiber breakage, and, ultimately, penetration of the material. On the other hand, in contrast to FRP composites, impact dents are formed that would reveal the impact during visual component inspections. Additionally, it was determined that Glare-5-2/1 laminates had the highest relative impact resistance of those tested.

Nomenclature

A	=	amplitude of oscillation
a	=	cylinder diameter
C_p	=	pressure coefficient
C_x	=	force coefficient in the x direction
C_y	=	force coefficient in the y direction
c	=	chord
$\mathrm{d}t$	=	time step
F_x	=	X component of the resultant pressure force acting on the vehicle
F_y	=	Y component of the resultant pressure force acting on the vehicle
f, g	=	generic functions
h	=	height
i	=	time index during navigation
j	=	waypoint index
K	=	trailing-edge nondimensional angular deflection rate

I. Introduction

MODERN aircraft structures use a wide variety of materials ranging from aluminum alloys to advanced composites. One new family of materials is being introduced into aircraft structures, fiber metal laminates (FMLs), which was conceived at the Delft University of Technology and Fokker Aircraft in the 1970s, 1980s and 1990s.[1–5] Early studies demonstrated the significant improvement in fatigue crack growth resistance vs monolithic aluminum that is obtained with FMLs. This improvement results from the "crack-bridging" effect, where intact fibers in the wake of fatigue cracks lower the effective crack tip stress intensity factor and reduce the crack growth rate. A typical FML, shown in Fig. 1, consists of thin layers of metal and fiber-reinforced polymer (FRP) bonded together and combines the beneficial features of monolithic metal alloys (machinability, formability, and impact tolerance) with those of composites (low density, good fatigue resistance, and manufacturing flexibility). Through the replacement of metal with lower density composite layers in FMLs, there is a reduction in overall density and, thus, a reduction in structural weight; this can reduce fuel consumption in transport aircraft.

FMLs are already being employed in next-generation civilian and military aircraft. For example, glass-reinforced aluminum (Glare) laminates have been produced for the upper fuselage sections on the Airbus A380 transport aircraft, and TiGr laminates of titanium and graphite-reinforced polymer are being considered for parts of the F-35 Joint Strike Fighter. Aramid-reinforced aluminum laminates (Arall) and Glare are already in use as secondary airframe structures, which are subject to impact loads, such as wing flaps.

Another important application of FMLs is as a replacement cargo liner material for regional and wide-body aircraft. The motivation is the lower maintenance cost because the FML liners are more resistant to impact damage than the fiberglass liners installed in many production aircraft. Additional benefits to using FMLs in this application include improved fire resistance and some explosion containment capability. Currently, the replacement FML liners are being installed in Bombardier Regional Jets and European ATR regional turboprop aircraft.

During regular operations, the primary and secondary structures of transport aircraft are often exposed to foreign object damage due to low-velocity impacts. In metallic airframes (especially ductile alloys such as aluminum 2024-T3), impact on exposed skins results in a plastically deformed dent. Aircraft structural repair manuals require dent repairs based on the dent size and location on the airframe. In contrast, conventional laminated composite material structures will typically show little evidence of a low-velocity impact; however, depending on the material, layup, and impact energy, significant internal delaminations may result and can substantially reduce the strength after impact.[6–8]

FMLs are known to behave similarly to monolithic aluminum alloys when subjected to low-velocity impacts in that they develop clearly visible dents when impacted. However, they are still laminated materials and, thus, can suffer from delaminations and

Received 5 January 2005; revision received 20 May 2005; accepted for publication 20 May 2005.

*Research Officer, Structures Group, 1200 Montreal Road, Building M3, Institute for Aerospace Research. Member AIAA.
†Professor, Department of Mechanical and Aerospace Engineering, 1125 Colonel By Drive.
‡Professor, Department of Aerospace Engineering, 350 Victoria Street.

cracking due to impact damage.[9–21] An extensive series of studies of this behavior has been carried out at the Technical University of Delft.[11–15] This previous work clearly identified the specific damage modes (delamination, cracking, and fiber fracture) formed as a result of low-velocity impact events as shown in Fig. 2. These studies also considered the relative impact performance of different types of FMLs.

In the time since these previous studies were conducted, numerous changes in the basic formulation of commercially available Glare laminates have taken place. Namely, the resin system was changed, and a standard laminate configuration was adopted for use in aircraft structures. Therefore, data from these previous tests could not be used to assess quantitatively the relative impact performance of the latest FML configurations. A new study was, thus, undertaken with Bombardier Aerospace to assess the impact performance of several specific types of Glare being considered for application in narrow-body regional aircraft applications. The technical objectives of the present investigation are as follows:

1) Review existing impact test methods for composites and FMLs to determine their suitability for the determination of the impact resistance of Glare laminates and, if required, design a new test method that minimizes the influence of fixture effects. This test method will provide a screening tool for different types of Glare laminates.

2) In a systematic way, examine the formation of impact damage in several types of commercially available Glare laminates being considered for possible application in aircraft fuselage structures.

3) Determine the relative impact performance of several types of commercially available Glare laminates.

4) Develop a detailed compendium of detailed impact loading curves that can be used for the validation of analytical or numerical impact models.

This paper is Part 1 of an extensive study of the effects of low-velocity impact on commercially available Glare laminates and deals with the experimental investigation of impact resistance. An overview of impact testing methods for FMLs will be presented with a summary of results from other researchers. This will be followed with a description of the test results including the quantitative impact damage resistance of FMLs and the impact damage geometry. A companion paper (Part 2) covers the development of a continuum damage mechanics-based impact damage model that was implemented in a commercially available finite element code, as well as a comparison between the results of experiments and simulations. Other work included investigations of postimpact damage tolerance of Glare under different loading conditions.[6] The study was carried out in collaboration between the Structures, Materials and Propulsion Laboratory (SMPL) of the Institute for Aerospace Research of the National Research Council of Canada (NRC–IAR), Carleton University, and Bombardier Aerospace.

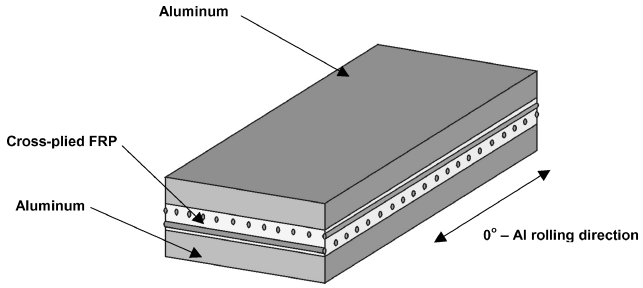

Fig. 1 Basic FLM configuration.

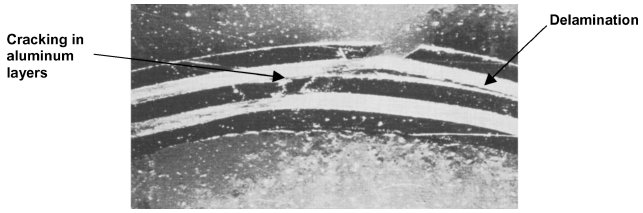

Fig. 2 Formation of impact-induced delamination and cracking in an Arall FML panel.[11]

II. Impact Testing

To evaluate the impact performance of FMLs, numerous impact studies have been conducted in the past on Glare and Arall laminates, as shown in Table 1. Because an FML is a laminated material, there were concerns that it could develop significant hidden internal damage, similar to FRPs, as shown in Fig. 3. Various impact test procedures have been used by different authors, many of them variations of existing methods for testing FRP composites. These tests typically use drop weight or pendulum impact devices for impact energy levels up to 70 J; higher impact energies and velocities require gas gun or other ballistic facilities. No single method has been standardized as yet for FMLs. A review of the previous test programs[11–21] showed that the specimen test area was generally small and, in several cases, rectangular or square. This finding raised a concern that the impact results could be affected by the specimen boundary support. It was decided to run a series of preliminary tests, to assess the boundary effects, and to establish impact energy levels for the Glare variants to be studied.

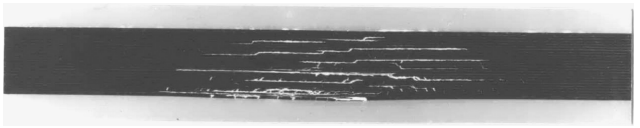

Fig. 3 Internal impact damage in conventional FRP laminate following low-velocity impact.[19]

Table 1 Summary of impact tests conducted on Glare and Arall[10-21]

Source	Materials tested	Test type	Impactor radius, mm	Coupon size, mm	Test area dimensions, mm
Ref. 10[a]	Glare	Drop	12.7 and 25.4	292 × 292	Diameter 203
Ref. 11	Arall and Glare	Drop	7.5 and 0.5	120 × 120	Diameter 80
Ref. 12	Arall and Glare	Drop	7.5	100 × 100	Diameter 80
Ref. 13	Glare	Drop	7.5	150 × 150	100 × 100
Ref. 13	Arall and Glare	Drop	5 and 7.5	100 × 100	Diameter 80
Ref. 14	Arall	Pendulum	7.5	125 × 125	100 × 100
Ref. 15	Arall and Glare	Drop	7.5	100 × 100	Diameter 80
Ref. 16	Arall	Drop	12.7	76 × 406	Diameter 50.8
Ref. 17	Arall	Pendulum	6.35	127 × 254	Not available
Ref. 18	Arall	Gas gun	6.35	101.6 × 25.4	Not available
Ref. 19	Arall	Gas gun	6.35	101.6 × 25.4	Not available
Ref. 20	Glare	Drop and bird	8.0	100 × 150	75 × 125
Ref. 21	Arall and Glare	Drop	8	100 × 100	Diameter 76

[a]Data discussed in present paper.

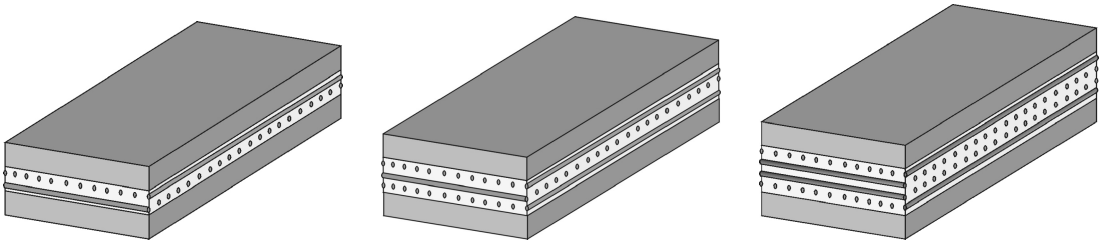

a) b) c)

Fig. 4 Schematic of laminates: a) Glare-3-2/1 ($t = 0.85$ mm), b) Glare-4-2/1 ($t = 0.98$ mm), and c) Glare-5-2/1 ($t = 1.11$ mm).

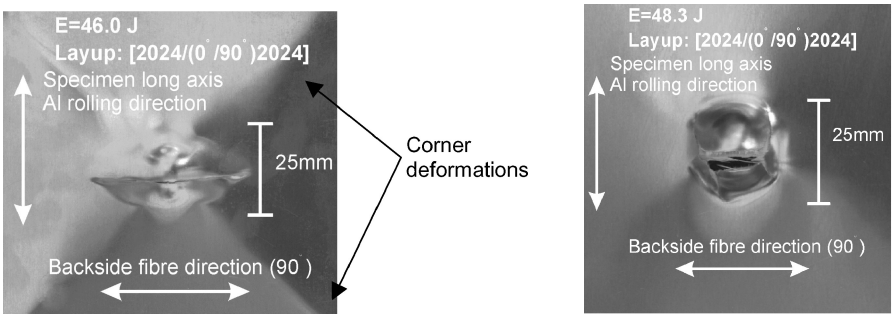

a) b)

Fig. 5 Impact damage in Glare-3-2/1 tested in a) NASA test fixture at 46.0 J and b) Carleton/SMPL test fixture at 48.3 J.

A. Glare Variants Tested

Three types of commercially available Glare-X-2/1 laminates, shown in Fig. 4, were selected for this study because they are potentially suitable for application in narrow-body, for example, regional or business, transport aircraft. In Fig. 4, the X in the laminate designation denotes the type of Glare and the 2/1 indicates that there are two layers of aluminum and one layer of FRP in the laminate.

B. Impact Test Method

Specimens were tested in a Dynatup drop weight impact tower at NRC–IAR. The impact tower system recorded the impact load through an instrumented impactor with a data acquisition system that is triggered by an infrared timing gate. This timing gate also gave the velocity of the crosshead at the moment of impact. Given the impact force history and the impact velocity, it is possible to calculate the impact energy, deflection, and velocity histories.

C. Preliminary Tests

Because of the laminated and hybrid nature of FMLs, they are classified as a type of composite material. Historically, composite materials have demonstrated poor impact performance with the formation of internal damage during impact loading. To develop a procedure for the impact testing of FMLs, a series of trial impact tests were conducted using two standard FRP composite impact fixtures with Glare-3-2/1 to assess the effect of fixture geometry on impact damage formation. These fixtures were originally developed by NASA and The Boeing Company and were chosen for the preliminary testing because they are widely accepted methods for testing the impact response of conventional composites.[22,23]

The trial tests demonstrated that the response to impact was influenced by the specimen test section configuration, rectangular (127×76 mm) for the Boeing test fixture and square (127×127 mm) for the NASA fixture. Figure 5a shows major corner deformations in a specimen supported in the NASA fixture. In response to this observation, a new fixture was designed and fabricated as shown in Fig. 6 (Ref. 6). The Carleton/SMPL fixture used a 292×292 mm square coupon with a 203-mm-diam test area. When this fixture was used, the observed specimen deformation and slippage were small and limited to the periphery of the specimens, well away from the central dent as shown in Fig. 5b. Because of the circular test area, there was a lack of corner deformations in the trial

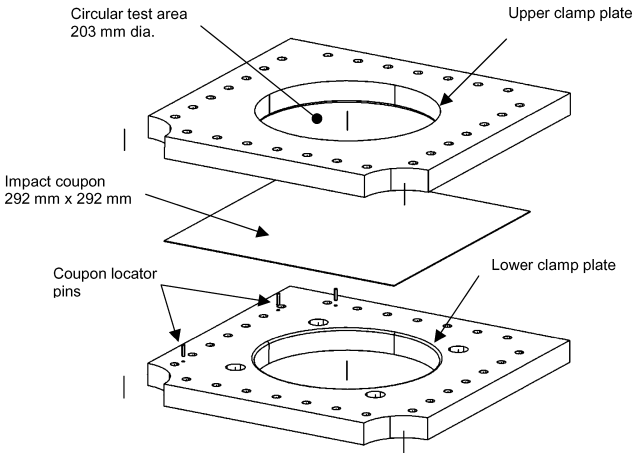

Fig. 6 FML-specific impact fixture developed at Carleton University and SMPL (Carleton/SMPL fixture).[6,7]

specimen tested in the new fixture near the same impact energy as the specimen tested previously in the NASA fixture. Thus, on the basis of these findings, it was concluded that the new fixture was suitable for the main test series.

To develop the full test matrix for the main series of impact tests, a further set of preliminary impact tests were conducted using the Carleton/SMPL fixture with a 25.4-mm impactor and a crosshead mass of 6.4 kg (Refs. 9 and 10). Each specimen was x rayed after impact to determine the extent of internal damage. This damage assessment enabled the selection of nominal impact energies E_{imp} for the test matrix (Table 2) for the main test series, representing impacts that would produce the following progressively increasing damage states: 1) plastically deformed dent with no delamination, typically for $E_{\text{imp}} \leq 20$ J; 2) plastically deformed dent with delamination, typically for $10 \text{ J} < E_{\text{imp}} < 55$ J); and 3) puncture, typically for $E_{\text{imp}} > 55$ J.

D. Experimental Results

The test matrix (Table 2) defined the nominal impact energy level for each batch of tests. There was typically a small difference between the nominal impact energy and the actual impact energy

Table 2 Test matrix for main series of Glare low-velocity impact tests[a]

Material	Thickness, mm	Areal density, kg/mm^2	Nominal impact energy level, J							Total
			15	25	35	45	55	60	65	
2024-T3	1.02	2.82	0	6	6	6	6	6	0	30
Glare-3-2/1	0.85	2.17	6	6	6	6	6	0	0	30
Glare-4-2/1	0.98	2.17	0	6	6	6	6	6	0	30
Glare-5-2/1	1.11	2.42	0	6	6	6	6	0	6	30
Total	n/a	n/a	6	24	24	24	24	12	6	120

[a]Impactor mass equal to 6.4 kg.

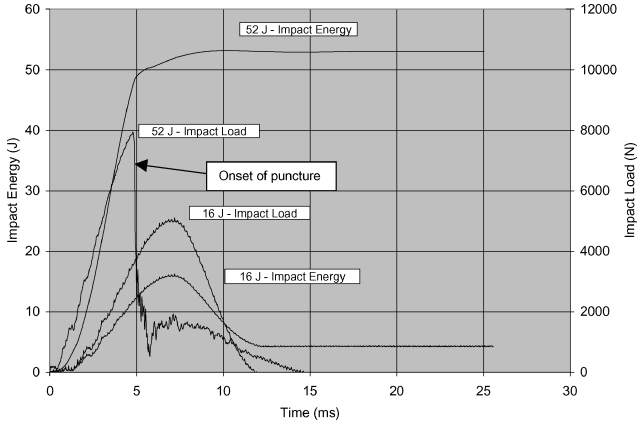

Fig. 7 Traces of impact energy and load vs time for Glare-3-2/1 impact tests with (specimen 44-52 J) and without puncture (specimen 36-16 J).

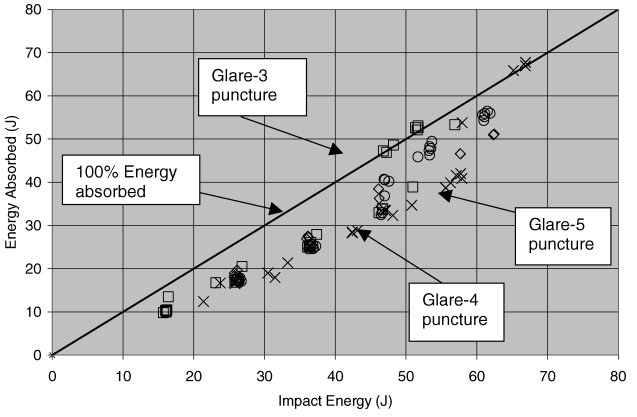

Fig. 8 Absorbed energy vs impact energy for Glare and 2024-T3: ◇, 2024-T3; □, Glare-3-2/1; ○, Glare-4-2/1; and ×, Glare-5.

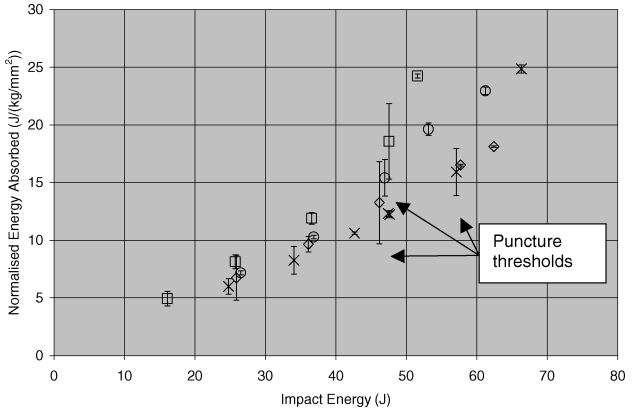

Fig. 9 Normalized absorbed energy vs impact energy; each data point an average of six tests: ◇, 2024-T3; □, Glare-3-2/1; ○, Glare-4-2/1; and ×, Glare-5-2/1.

computed by the Dynatup system. Because the actual impact energy was calculated from the velocity measured at the moment of impact, it was used in all analyses presented herein. The experimental results will be described beginning with the force and energy histories for typical impact events. Following this, the results of the posttest inspections will be discussed.

Figure 7 shows typical energy and load histories for two representative Glare-3-2/1 panels above and below the puncture threshold. For impact events below the puncture threshold, some energy is returned to the crosshead during rebound and the remainder is absorbed through plastic deformation, delamination, and matrix cracking. The onset of puncture can be identified by the sharp drop in the impact force, as indicated in Fig. 7. The impact energy is not recovered following the puncture because it is almost fully converted to plastic deformation, internal damage, and cracking. In cases where the crosshead passed through the specimen, some kinetic energy is retained by the crosshead; these extreme puncture events are excluded from the analysis.

The relative impact performance of the different types of Glare may be compared by considering several parameters including the absorbed energy, the peak impact force, and the dent depth. The amount of energy absorbed by the panel as a function of impact energy is shown in Fig. 8. The absorbed energy increases with increasing impact energy but, before puncture, the amount of absorbed energy is below the impact energy. The unabsorbed energy is transferred back to the impactor, which then rebounds. When the specimens are punctured, there is a jump in the amount of energy absorbed by the specimen as indicated in Fig. 8. Overall, impact energy is absorbed by several mechanisms: 1) plastic deformation of the panel and matrix cracking, 2) delamination damage, 3) fiber and aluminum fractures as the panels are punctured by the impactor, and 4) convertion to sound and heat[10] of a small portion.

It is not possible to determine from these experiments the exact amounts of energy absorbed by these mechanisms; however, impact simulations can provide estimates of the different components of absorbed energy.

To examine the relative performance of the different types of Glare, a graph was prepared where the absorbed energy was normalized in terms of the areal density (mass per unit area) of the panels as shown in Fig. 9. To prepare this graph, each group of six impacted specimens was averaged for each impact energy level. The vertical error bands for each data point indicate a single standard deviation in the data. The data points for Glare-3-2/1, Glare-4-2/1, and Glare-5-2/1 with relatively large error bands are specimens where the impact energies were at the puncture threshold. Near the puncture threshold, each averaged batch of data may contain specimens in which puncture occurred and some in which puncture did not occur. Note that Glare-5-2/1 absorbed the least amount of energy for its areal density and, therefore, suffered the least amount of damage. The additional layers of FRP in Glare-5-2/1 increased its impact resistance while decreasing the areal density of the laminates.

The peak impact force as a function of impact energy is shown in Figs. 10 and (normalized) 11. As shown in Figs. 10 and 11, the impact force varies almost linearly with the energy. However, at higher impact energies, the impact force levels off in Glare-3-2/1 and Glare-4-2/1, but not in Glare-5-2/1 punctured panels. Of the FML panels, Glare-5-2/1 had the lowest normalized peak impact force

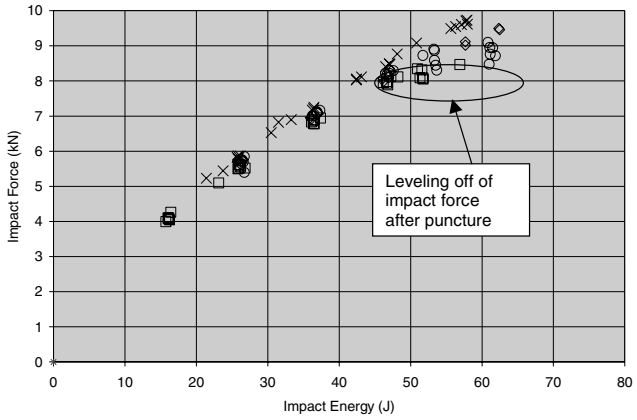

Fig. 10 Peak impact force vs impact energy: ◇, 2024-T3; □, Glare-3-2/1; ○, Glare-4-2/1; and ×, Glare-5-2/1.

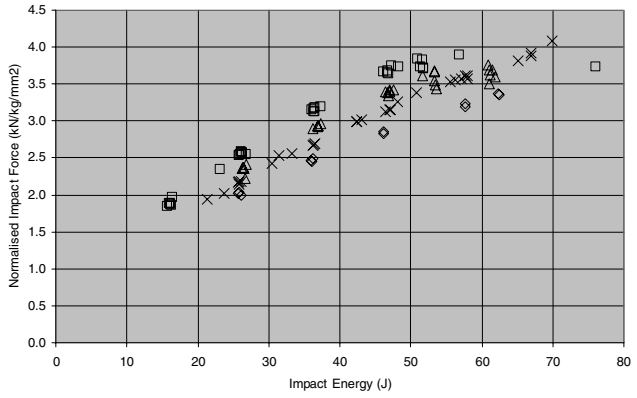

Fig. 11 Normalized peak impact force vs impact energy: ◇, 2024-T3; □, Glare-3-2/1; △, Glare-4-2/1; and ×, Glare-5-2/1.

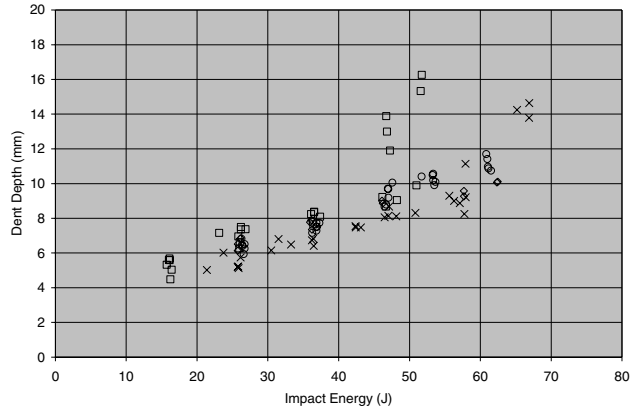

Fig. 12 Permanent dent depth vs impact energy: ◇, 2024-T3; □, Glare-3-2/1; ○, Glare-4-2/1; and ×, Glare-5-2/1.

with respect to impact energy due to the higher relative amount of FRP in the panel.

E. Impact Damage Formation

Typical composite materials can develop substantial internal damage under impact loading in the form of delamination and matrix cracks. An extensive series of destructive and nondestructive postimpact inspections were carried out on the impacted FML panels to determine if similar damage modes existed. Also, a study of the dent depth as a function of impact energy was conducted to compare FMLs to monolithic metals. This analysis of damage modes began with visually observed damage, that is, puncture and dent depth, and then proceeded to an investigation of the internal damage in the FML panels. The effect of the layup on the observed damage modes was also analyzed.

Figure 12 shows the permanent dent depth vs impact energy for all of the materials tested. The dent depth was measured with a Vernier depth gauge (±0.025 mm) relative to the undeformed edge of the specimen. The Glare-5-2/1 laminates had the lowest permanent deformations, which was due in part to the higher proportion of FRP layers. The fibers in these layers resisted permanent deformation; thus, as this proportion increased, the overall permanent deformation of the laminate decreased. The sharp increase in dent depth for the Glare-3-2/1 material was caused by the formation of deep through punctures in the panels.

To determine whether dent depth was an appropriate measure of the extent of internal damage below the puncture threshold, it will be necessary to conduct an additional study linking delamination size to dent depth. The present study focused on the geometry and extent of puncture damage in the impacted FMLs. Figures 13–15 show typical examples of puncture damage in Glare panels and how it was influenced by the fiber orientations in the panels. (E_{imp} is the impact energy.) Both the Glare-3-2/1 and Glare-5-2/1 laminates had an equal proportion of fibers in the 0- and 90-deg directions, as shown in Fig. 3. This layup resulted in puncture cracks that were oriented in these two directions (Figs. 13 and 15). Glare-4-2/1 has 70% of its fibers in the 0-deg direction, parallel to the rolling direction of the aluminum sheets. Thus, when puncture occurred, only a single crack oriented in the 0-deg direction was formed, as shown in Fig. 14. Note that the crack length was a direct function of the impact energy, as indicated in Fig. 16.

Figures 17–28 show the typical damage modes observed in destructive cross sections of the Glare specimens as compared to nondestructive dye penetrant enhanced x rays. Figures 17–28 show the progression, type, and extent of damage in Glare-3-2/1, Glare-4-2/1, and Glare-5-2/1, as well as a comparison of damage that was revealed using the nondestructive and destructive inspection techniques. Dye penetrant enhanced x ray was selected over ultrasonic methods based on information in literature that described the ineffectiveness of ultrasonic methods in determining the extent of internal damage in impacted FMLs.[8–10] To conduct the x-ray inspections, an x-ray opaque dye was introduced by drilling a small hole in the center of the impact dent and then injecting the dye into the impacted layers.

A dye penetrant enhanced x ray of the Glare-3-2/1 sample 31, which was impact tested at 16 J and is shown in Fig. 17a, did not indicate the presence of delamination damage. However, the cross

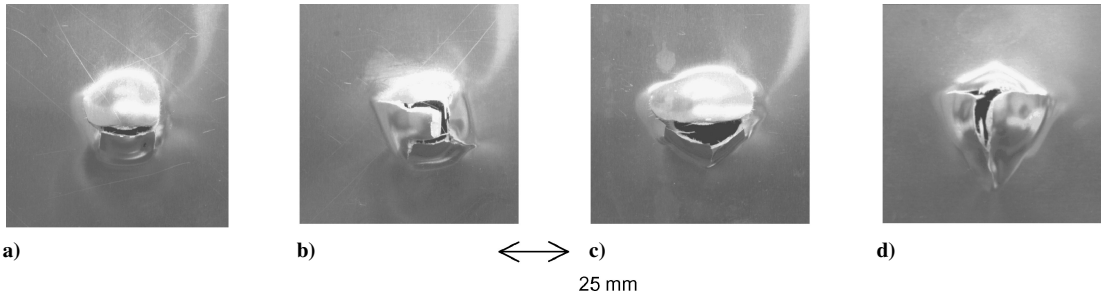

Fig. 13 Puncture damage in Glare-3-2/1: a) specimen 14, $E_{\text{imp}} = 47$ J; b) specimen 15, $E_{\text{imp}} = 52$ J; c) specimen 25, $E_{\text{imp}} = 52$ J; and d) specimen 35, $E_{\text{imp}} = 51$ J.

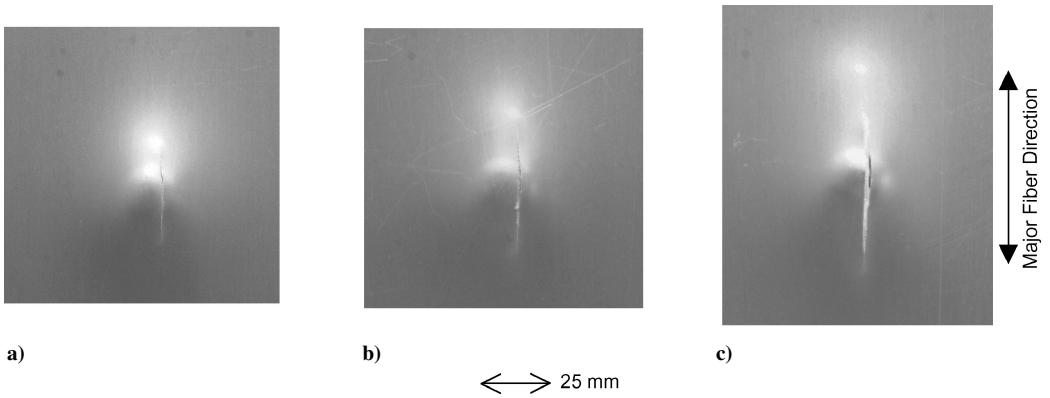

Fig. 14 Puncture damage in Glare-4-2/1: a) specimen 08, $E_{imp} = 47$ J; b) specimen 09, $E_{imp} = 54$ J; and c) specimen 10, $E_{imp} = 61$ J.

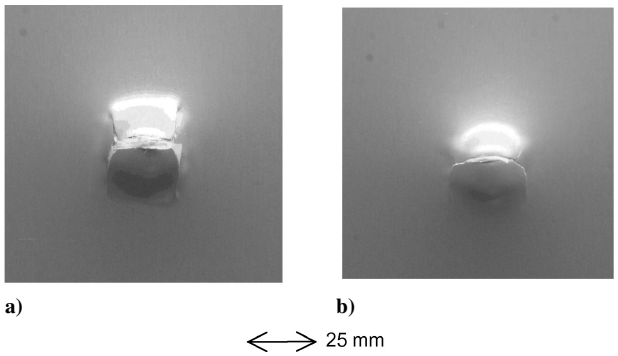

Fig. 15 Puncture damage in Glare-5-2/1: a) specimen 14, $E_{imp} = 58$ J and b) specimen 10, $E_{imp} = 67$ J.

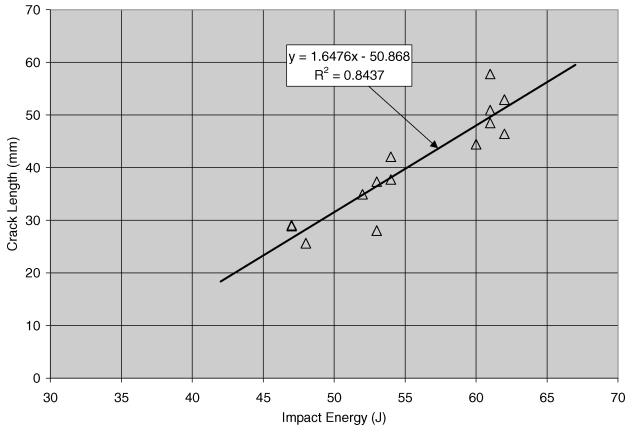

Fig. 16 Crack length in partially punctured Glare-4-2/1 coupons vs impact energy.

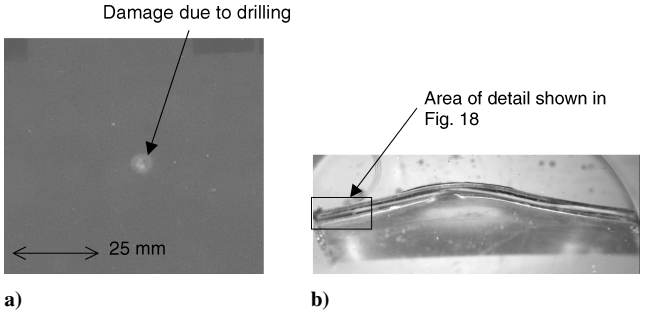

Fig. 17 Sample Glare-3-2/1 specimen 31 (16 J): a) x ray and b) cross section.

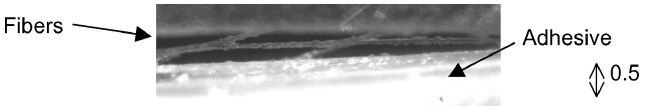

Fig. 18 Glare-3-2/1 specimen 31 (16 J) fiber bridging.

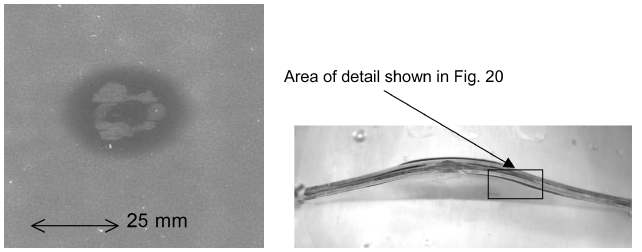

Fig. 19 Glare-3-2/1 specimen 33 (36 J): a) x ray and b) cross section.

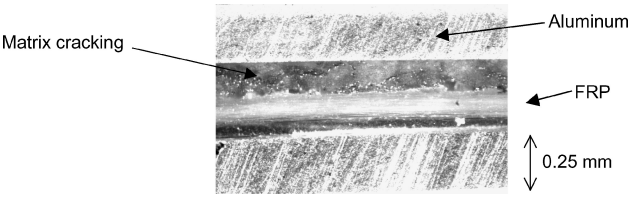

Fig. 20 Matrix cracking in Glare-3-2/1 specimen 33 in 90-deg layer.

section, Fig. 17b, revealed delamination damage throughout the impacted area. A detailed examination showed that the fiberglass layers near the impacted surface of the panel were intact and were adhering to the aluminum layer, preventing the flow of the penetrant to the damage. This indicates that even the x-ray-based technique may be limited in effectiveness for inspecting impacted FMLs. This specimen developed fiber bridging from the impact as shown in Fig. 18.

An x ray of Glare-3-2/1 specimen 33 (36 J) shown in Fig. 19a revealed delamination damage from the impact. The dye penetrant was able to infuse the full extent of the delaminated region; therefore, the destructive inspection (Fig. 19b) agreed with the x-ray results. The sample also had matrix cracking (Fig. 20) that was not observed using x rays. This cracking occurred between the fibers of the 90-deg layer with no damage observed in the 0-deg layer.

The Glare-4-2/1 specimens showed substantially different impact damage modes when compared to the Glare-3-2/1 specimens. Sample Glare-4-2/1 specimen 08 (47 J) shown in Figs. 21–23 developed a through crack in addition to the delamination damage. It was also noted that the fibers in the 0-deg direction were fractured when the through crack formed. The panel suffered extensive delamination (Fig. 22a) and matrix cracking (Figs. 22b, 22c, and 23). The offset between the two halves of the crack occurred after the specimen was cut from the impacted panel and the stored elastic energy was released. It was not possible to determine whether this release of energy increased the size of the observed delaminated region.

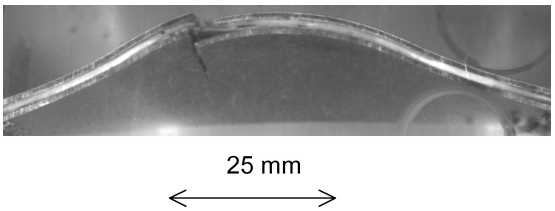

Fig. 21 Glare-4-2/1 specimen 08 (47 J) cross section.

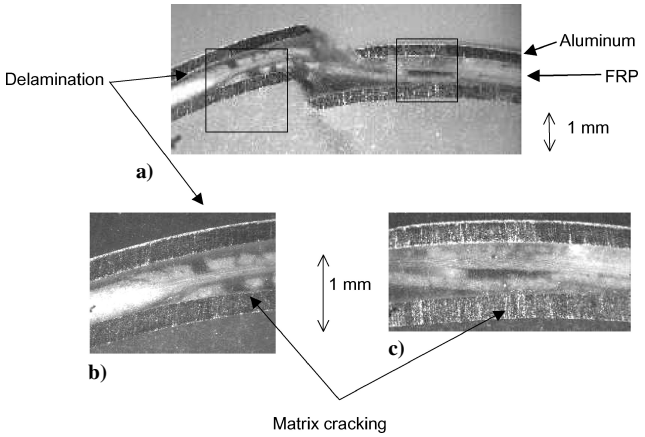

Fig. 22 Glare-4-2/1 specimen 08 (47 J): a) through crack and b) and c) matrix cracking.

Fig. 23 Matrix cracking in Glare-4-2/1 specimen 08 (47 J).

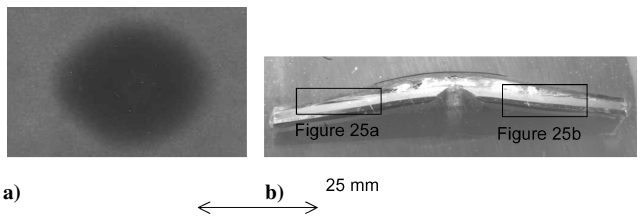

Fig. 24 Glare-5-2/1 specimen 04 (58 J): a) x ray and b) cross section.

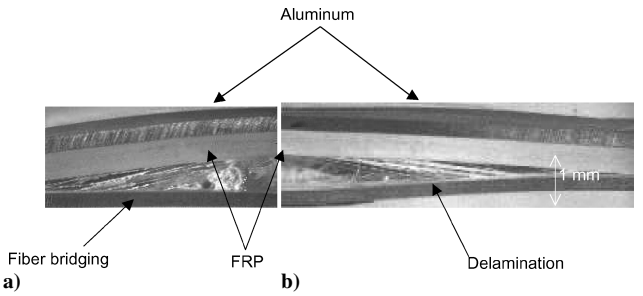

Fig. 25 Delamination and fiber bridging in Glare-5-2/1 specimen 04 on a) left and b) right of dent.

The Glare-5-2/1 specimens exhibited damage modes similar to those observed in the Glare-3-2/1 specimens. There were also instances where the x-ray inspections did not reveal the full extent of the internal delaminations. Glare-5-2/1 sample 04 (58 J) showed considerable delamination damage as shown in Figs. 24a and 24b. In this case, the x ray (Fig. 24a) and the cross section (Fig. 24b) agreed. Significant delamination was noted at the edge of the dent (Figs. 25a and 25b). This sample also contained extensive matrix cracking (Fig. 26).

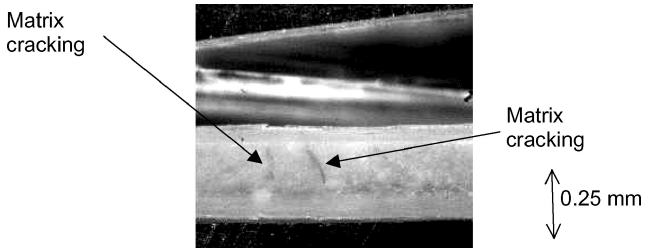

Fig. 26 Matrix cracking in Glare-5-2/1 specimen 04.

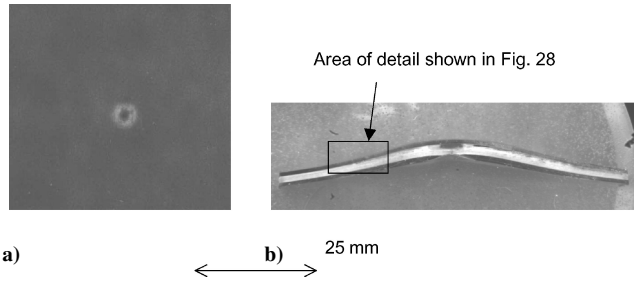

Fig. 27 Glare-5-2/1 sample 12 (36 J): a) x ray and b) cross section.

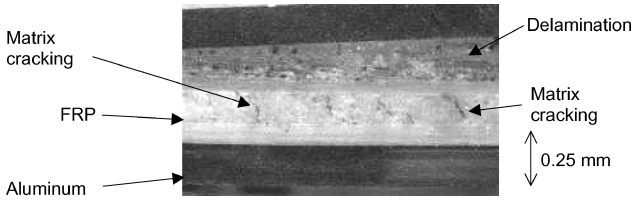

Fig. 28 Glare-5-2/1 sample 12 matrix cracking and delamination.

Glare-5-2/1 sample 12 (36 J) shown in Figs. 27 and 28 developed delamination damage that was not apparent in the x rays. This specimen provides a further example of the type of matrix cracks typical of all of the specimens inspected (Fig. 28).

It has been previously demonstrated that in impacted FMLs interlaminar shear forces between the aluminum and fiberglass layers are responsible for the onset of delamination damage.[11] The initiation of the delamination process is controlled by mode 2 (in-plane shear) stresses between the plies. This leads to the formation of matrix cracks during the early stage of the impact event. These cracks then provide the nucleation sites for delamination as the impactor rebounds due to mode 1 (opening) stresses between the plies. The plastically deformed aluminum layers pull away from one another, causing regions of delamination to open up around the dent. Further study and analytical modeling is required to determine the relative contribution of modes 1 and 2 stresses and their progression during delamination formation in FMLs.

III. Discussion

The impact tests conducted as part of this work provided several insights into the development of impact-induced damage in FMLs. The specific types of damage varied with the impact energy as follows:

1) A plastically deformed dent with no delamination occurred generally below 10 J.

2) The formation of internal delaminations and matrix cracking with damage becoming visible in penetrant enhanced x rays; begins between 10 and 15 J.

3) Partial puncture occurs in Glare-4-2/1 laminates only.

4) Puncture occurs with the geometry of the puncture dependant on the Glare layup, as will be discussed.

Note that the specific energy thresholds will vary with the type of laminate and also with the boundary conditions of the fixture. However, for coupon-level impact events, the general damage progression will proceed in the same manner as just outlined.

The Glare layup strongly influenced the resulting damage geometry, as shown by the formation of a single crack oriented parallel to the major fiber direction in all of the Glare-4-2/1 specimens. If Glare-4-2/1 structures are designed appropriately, then the detrimental effect of this type of impact crack may be reduced. For example, if the postimpact load was unidirectional and parallel to the crack direction, then the impact-induced cracks in Glare-4-2/1 would not grow. However, in the majority of applications, such as fuselage or wing skins, the applied loads on the laminate are not uniaxial but have an off-axis resultant and would cause crack growth. For example, as was described in Ref. 21, impact-induced cracks oriented at 45 deg to the loading axis were observed to grow under constant amplitude loading. In Glare-3-2/1 and Glare-5-2/1, multiple cracks formed as a result of impact, and the damage did not change appreciably in size once the panel was punctured.

It was also found that when puncture occurred in the Glare-3-2/1 and Glare-5-2/1 laminates, the impactor did not rebound, and thus, the panel absorbed all of the impact energy up to a certain limit, approximately 80 J. Beyond this limit, the impactor would pass through the panel and the remaining kinetic energy would be absorbed by the structure of the drop tower when the crosshead was arrested by the rubber stops. On an areal density basis, the Glare-5-2/1 laminates absorbed less energy than Glare-3-2/1, Glare-4-2/1, and 2024-T3 when subjected to low-velocity impact. This was due to the larger amount of glass fibers in the 0- and 90-deg directions of the impact-optimized Glare-5-2/1 laminates, compared to Glare-3-2/1 and Glare-4-2/1.

Because only Glare-X-2/1 laminates were available for these tests, other types of Glare should be subjected to impact loading in the future. In particular, an examination of the influence of the number of layers on the formation of impact damage in thicker laminates would be desirable.

The nondestructive inspection technique used to examine the impact Glare panels accurately revealed the delaminations in specimens impacted at energies greater than 35 J. At lower energy levels, this technique did not expose the delamination damage because the damage was not connected to the small hole feeding dye-penetrant fluid into the material. With some modifications to the technique, such as the use of multiple holes, it may be possible to infiltrate the damaged regions fully. The destructive inspection technique accurately depicted the damage in the specimens; however, this method is laborious and limited in providing a damage map by the selected cutting geometry. Additional technologies should be investigated for application to the nondestructive inspection of impacted FMLs. These could include contact c-scan ultrasonic probes and laser ultrasound. For operational use, criteria relating the internal damage to the visible evidence, such as the dent depth, would provide guidance to the damage assessment similar to that used in the current metallic airframes. Note that all of the types of specimens showed significant matrix cracking in the nonpunctured panels. This form of damage contributed to the overall energy absorption of the impacted panels. Significant fiber fracture was only observed in panels that had been punctured.

These tests demonstrated the improved impact performance of FMLs as compared to conventional composites. Even at very low energy levels, a clearly visible dent is formed in the FML panels, whereas in conventional composites there is the possibility of hidden internal damage. Additionally, when compared to monolithic 2024-T3, a standard aircraft skin material, under impact loading, FMLs performed favorably and displayed similar, or in some cases better, impact resistance.

The impact test results provide a useful database for the versions of Glare that were studied. When the amount of work associated with the testing, data analysis, and nondestructive/destructive inspections is considered, it was felt that it would be advantageous to develop a method to predict the damage due to impact in FMLs. In conjunction with a limited amount of testing for each investigated FML, such a method would be highly cost effective in design and analyses of FML components.

IV. Conclusions

An extensive series of impact tests on Glare laminates 3-2/1, 4-2/1, and 5-2/1 has been carried out. This program successfully met all of the technical objectives established at its outset. The developed impact test method was used successfully to screen several varieties of commercially available Glare laminates to assess their relative impact performance. Additional conclusions that can be drawn from the test program are as follows:

1) Impact test fixture configuration must be carefully selected to avoid the influence of the coupon boundaries on the behavior of the material under impact.

2) Glare-5 absorbs less impact energy and, thus, suffers less damage, on an areal density basis than aluminum 2024-T3, Glare-3, or Glare-4 because of its greater volume fraction of fibers. As a result, it appears to be more suitable for applications where impact loading is an important design criterion.

3) The orientation of a majority of the fibers in the 0-deg direction results in the formation of a single crack in punctured Glare-4 specimens. This crack increases in size with increasing impact energy. In the other Glare variants, the cracks developed in the 0- and 90-deg fiber directions and did not increase in size with increasing impact energy.

4) Dents formed in Glare during impact are clearly visible and will increase the probability of detection of impact events, in comparison with composite materials.

It is highly desirable to develop a methodology for numerically simulating the impact, to enable the determination of internal damage in FMLs.

Acknowledgments

The authors wish to express their appreciation to Bombardier Aerospace for supplying the Glare laminates used in this study and for providing partial funding for this project and to the technical staff of the Institute for Aerospace Research–Structures, Materials and Propulsion Laboratory for their assistance and expertise.

References

[1]Vogelsang, L. B., Marissen, R., and Schijve, J., "A New Fatigue Resistant Material: Aramid Reinforced Aluminum Laminate (ARALL)," 11th Symposium of the International Committee on Aeronautical Fatigue, May 1981.

[2]Gregory, M. A., and Roebroeks, G. H. J. J., "Fiber Metal Laminates: A Solution to Weight, Strength and Fatigue Problems," *30th Annual Canadian Institute of Mining, Metallurgy and Petroleum Conference of Metallurgists*, National Research Council, Ottawa, 1991, pp. 43–56.

[3]Asundi, A., and Choi, A. Y. N., "Fiber Metal Laminates: An Advanced Material for Future Aircraft," *Journal of Materials Processing Technology*, Vol. 63, No. 1, 1997, pp. 386–394.

[4]Vlot, A., and Gunnink, W., *Fiber Metal Laminates: An Introduction*, Kluwer Academic, Dordrecht, The Netherlands, 2001, Chap. 1.

[5]Vlot, A., *Glare: History of the Development of a New Aircraft Material*, Kluwer Academic, Dordrecht, The Netherlands, 2001, Chap. 2.

[6]Brewer, J. C., and Lagace, P. A., "Quadratic Stress Criterion for Initiation of Delamination," *Journal of Composite Materials*, Vol. 22, Dec. 1988, pp. 1141–1155.

[7]Choi, H. Y., and Chang, F.-K., "A Model for Predicting Damage in Graphite/Epoxy Laminated Composites Resulting from Low-Velocity Point Impact," *Journal of Composite Materials*, Vol. 26, No. 14, 1992, pp. 2134–2169.

[8]Majeed, O., Worswick, M. J., Straznicky, P. V., and Poon, C., "Numerical Modelling of Transverse Impact on Composite Coupons," *Canadian Aeronautics and Space Journal*, Vol. 40, No. 3, 1994, pp. 99–107.

[9]Laliberté, J., Poon, C., and Straznicky, P. V., "Durability Testing of Fiber Metal Laminates," Inst. for Aerospace Research, Rept. IAR-LTR-ST-2231, National Research Council, Ottawa, Oct. 1999.

[10]Laliberté, J., "Investigation of Low-Velocity Impact Damage in Fiber Metal Laminates," Ph.D. Dissertation, Dept. of Mechanical and Aerospace Engineering, Carleton Univ., Ottawa, Nov. 2002.

[11]Vlot, A., "Impact Tests on Aluminum 2024-T3, Aramid and Glass Reinforced Laminates and Thermoplastic Composites," Delft Univ. of Technology, Rept. LR-534, Delft, The Netherlands, 1987.

[12]Vlot, A., "Low-Velocity Impact Loading on Fiber Reinforced Aluminum Laminates (ARALL and Glare) and Other Aircraft Sheet Materials,"

Delft Univ. of Technology, Rept. LR-718, Delft, The Netherlands, March 1993.

[13]Vlot, A., "Impact Properties of Fiber Metal Laminates," *Composites Engineering*, Vol. 3, No. 10, 1993, pp. 911–924.

[14]Vlot, A., "Impact Loading on Fiber Metal Laminates," *Journal of Impact Engineering*, Vol. 18, No. 3, 1996, pp. 291–308.

[15]Vlot, A., Kroone, E., and Larocca, G., "Impact Response of Fiber Metal Laminates," *Key Engineering Materials*, Vol. 141–143, 1998, pp. 235–276.

[16]Johnson, W. S., "Impact and Residual Fatigue Behavior of ARALL and AS6/5245 Composite Materials," NASA Langley Research Center, TM 89013, Oct. 1986.

[17]Hoogsteden, W. P., "Compression After Impact Behavior of ARALL®-1 Laminates," Wright Lab., Rept. WL-TR-91-4090, Wright–Patterson AFB, OH, July 1992.

[18]Wu, H. F., and Sun, C. T., "Impact Damage Characterization of Aramid Aluminum Laminates," *9th International Conference on Composite Materials*, Vol. 4, Woodhead Publishing, Ltd., Cambridge, England, U.K., 1993, pp. 157–165.

[19]Sun, C. T., Dicken, A., and Wu, H. F., "Characterization of Impact Damage in ARALL Laminates," *Composites Science and Technology*, Vol. 49, No. 2, 1993, pp. 139–144.

[20]Poston, K., "Impact Properties and Related Applications of Fiber Metal Laminates," Structural Laminates Corp., Rept. TD-M-94-007, Delft, The Netherlands, June 1994.

[21]Liaw, B. M., Liu, Y. X., and Villars, E. A., "Impact Damage Mechanisms in Fiber-Metal Laminates," *SEM Annual Conference*, Society for Experimental Mechanics, Bethel, CT, 2001, pp. 536–539.

[22]"Advanced Composite Compression Tests," The Boeing Co., Boeing Specification Support Standard 7260, Seattle, WA, 1988.

[23]"Standard Tests for Toughened Resin Composites," Aircraft Energy Efficiency Composites Project Office, NASA RP 1092, 1983, pp. 1–6.

A. Palazotto
Associate Editor